UNIVERSIDAD NACIONAL DE COLOMBIA
SEDE MEDELLÍN
FACULTAD DE MINAS

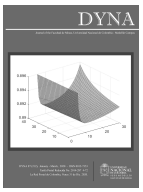

DYNA
http://dyna.medellin.unal.edu.co/

Design of an antenna array for a LFM-CW synthetic aperture radar prototype

Alfonso Zozaya [a] & Paulino Del Pino [b]

[a] Departamento de Electricidad. Universidad Tecnológica Metropolitana del Estado de Chile (UTEM), Santiago, Chile. a.zozayas@utem.cl
[b] Laboratorio de electromagnetismo aplicado LABEMA. Facultad de Ingeniería. Universidad de Carabobo. Valencia, Venezuela. pdelpi@gmail.com

Received: June 10th, 2019. Received in revised form: December 16th, 2019. Accepted: January 13th, 2020.

Abstract
This paper deals with the design of two identical 1 × 4 patch antenna arrays for a linear frequency modulated (LFM) continuous wave (CW) synthetic aperture radar (SAR) prototype. The theoretical design is carried out by using the empirical equations available in the literature, while the design optimization is performed by numerical methods using two commercial full wave simulators. Once the antennas are built they are experimentally characterized and incorporated into a radar prototype implemented at the Ecuadorian Space Institute. The radar is tested in a probing polygon and the horizontal resolution is estimated. A measured azimuthal resolution value very close to the theoretical one is achieved.

Keywords: Synthetic Aperture Radar (SAR); patch antenna array; radar.

Diseño de un arreglo de antenas para un prototipo de radar de apertura sintética LFM-CW

Resumen
Este artículo trata sobre el diseño de dos arreglos idénticos de 1 × 4 antenas de microcinta para un prototipo de radar de apertura sintética (SAR) de onda continua (CW) y con modulación lineal de frecuencia (LFM). El diseño teórico se lleva a cabo mediante el uso de las ecuaciones empíricas disponibles en la literatura, mientras que la optimización del diseño se realiza mediante métodos numéricos utilizando dos simuladores comerciales de onda completa. Una vez que se construyen las antenas, estas se caracterizan experimentalmente y se incorporan luego a un prototipo de radar implementado en el Instituto Espacial Ecuatoriano (IEE). El radar se prueba en un polígono y sobre la imagen procesada se estima la resolución horizontal. Se obtiene un valor de resolución azimutal medido muy cercano al teórico.

Palabras clave: Radar de Apertura Sintética (SAR); arreglo de antenas de microcinta; radar.

1. Introduction

There is a wide literature reporting the usefulness and effectiveness of synthetic aperture radar (SAR) in diverse fields, including climate monitoring, seas, terrestrial ice layers, mining, topographic surveys, land classification, hydrocarbon pollution monitoring, global positioning systems, among others [1]. The principle of operation of SAR systems can be summarized as the construction of images by phase discrimination between the microwave pulse signals transmitted and received by the radar when they are incident and reflected by the surface of an object under study [2-5].

Among the various technological aspects that should be addressed in designing and implementing SARs, the design of transmitting and receiving antennas is an important one. In general it is required that these antennas are small, lightweight, low cost, have good performance and be easy to manufacture. This makes microstrip antennas excellent candidates for SARs.

One of the main goals of the antenna design is to obtain a radiation pattern that exhibits a horizontal beamwidth that leads to an azimuthal spatial resolution appropriate for the

How to cite: Zozaya, A. and Del Pino-Pettinare, P, Design of an antenna array for a LFM-CW synthetic aperture radar prototype. DYNA, 87(212), pp. 96-101, January - March, 2020.

purposes of the radar [1-7]. Other important figures of merit for the antenna are return loss, polarization purity, power, and gain.

In this article, we describe the designing of two identical 1 × 4 patch antenna arrays to be incorporated in a linear frequency modulated (LFM) continuous wave (CW) synthetic aperture radar prototype implemented at the Ecuadorian Space Institute (IEE). We aim with this work to achieve a very important expertise in the area of antenna engineering for synthetic aperture radars within the Instituto Espacial Ecuatoriano, that permit us to trace a roadmap for designing and implementing, in a medium to long-term, an operative radar for remote sensing purposes. The main goal of the project is to obtain a horizontal beamwidth of $\Delta\theta_H \approx 24°$ in order to achieve an azimuthal resolution better than 20 cm.

At first, the antennas were designed using its transmission lines theoretical model [7-9]. Later on, the resulting geometry was optimized using the High Frequency Electromagnetic Field Simulation (HFSS) of Ansys [10] and the Advanced Design System (ADS) from Agilent [11].

We used an inset to feed the patches, and T-Junctions and λ/4 adapters to feed the array [9,12].

Once the antennas were fabricated, we measured the return loss (*RL)*, the standing wave ratio (*SWR)*, the resonance frequency (f_0), the bandwidth (*BW)*, the gain, and the radiation pattern.

Finally, we incorporated the antennas into the radar and made measurements on a test polygon. We estimated the cross-range spatial resolution and found good agreement with the theoretically expected value.

The rest of this article is structured as follows: in Section 2 we describe the antennas design procedure and we present some simulation results. In Section 3 we describe the experimental characterization results of the constructed antennas. In Section 4, we briefly analyze the antenna's performance, once incorporated to the radar, and finally in Section 5 we give some conclusions.

2. Antenna design and optimization

2.1. Substrate selection and base antenna design

The geometry of the array base antenna is shown in Fig. 1. The base antenna consists of a thin rectangular film of conductive metal of thickness *t*, width *W* and length *L*, on a dielectric substrate of thickness *h* and dielectric constant ε_r, resting on a broad conductive metal film that serves as a ground plane.

Many substrates are commercially available for designing a microstrip antenna. The dielectric constant of these substrates can vary from a minimum of 2.2 to a maximum of 12: $2.2 < \varepsilon_r < 12$. According to [8], a dielectric constant close to the lower limit of 2.2 and a high thickness provide the best bandwidth and the best performance, even though at the expense of a larger size. So, to favor the efficiency of the antenna we have chosen a dielectric constant of $\varepsilon_r = 3.5$ as initial guess. To settle the thickness *h* of the substrate the

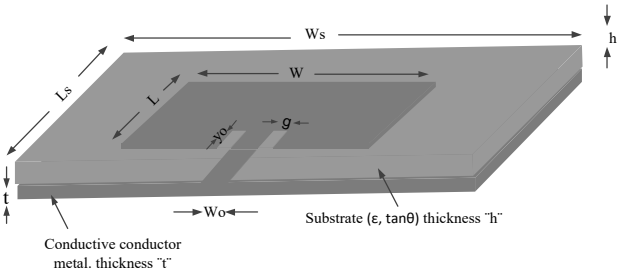

Figure. 1. Inset-fed patch antenna used as the array base antenna. Source: The Authors.

bandwidth of the radar was taken into account. The central operating frequency of the radar is f_0 = 2.44 GHz and the expected bandwidth is of about 24 MHz (1% of f_0). From the information contained in Fig. 2 of [13], best reproduced as Fig. (14.27) on page 854 of [8], we have determined that a minimum substrate thickness *h* of approximately $0.012\lambda_0$, or $h = 1.48\ mm$, is required to achieve such a bandwidth for a dielectric constant of 3.5. These guess values ($\varepsilon_r = 3.5$ and $h = 1.48\ mm$) served for searching a commercially available substrate. After consulting the Rogers database [14] we have selected the RO4003C substrate ($\varepsilon_r = 3.55$, $h = 1.524$ mm) for the project.

Given the selected substrate, we have designed the base patch antenna theoretically using the equations derived from the Transmission Line Theory as described in Reference [8], pages 817-820: equations (14.1), (14.2), (14.5), (14.6) and (14.7). The design equations given in [8] were transcribed directly in a GNU Octave script for a resonance frequency f_0 = 2.44 GHz. By the other hand, we calculated the minimum dimensions of the substrate, W_s and L_s, according to [15] as:

$$W_s = W + 6h \quad (1)$$

$$L_s = L + 6h \quad (2)$$

By the way, we have calculated the insertion point y_0 of the feeding strip in the patch, its width W_0 and its separation *g* from the antenna using the equations available in [8,16].

2.2. 1 × 4 patch-antennas array design

We designed a broadside horizontal array of 4 elements using the equation for the theoretical array factor given in [8] using GNU Octave. We carried out some iterations for the separation *d* between two successive base antennas until a theoretical horizontal beamwidth of $\Delta\theta_H \approx 24°$ was obtained.

We used three T-junctions to feed the array as shown in Fig. 2. Each T-junction is made of a 50 Ω line connected to two 70.7 Ω lines. The 70.7 Ω lines have been cut to a length of 1.92 mm (λ / 4) to properly transform 50 Ω to 100 Ω. A chamfer of 3.8266 mm was made in the outer corner of right angles in all the 50 Ω lines. We calculated the chamfer length as √2 x, where $x = D \times M / 100$, *D* is the length of the diagonal of the corner and *M* is determined, for $wl/h \geq 0.25$ and $\varepsilon_r < 25$, as [9,13]:

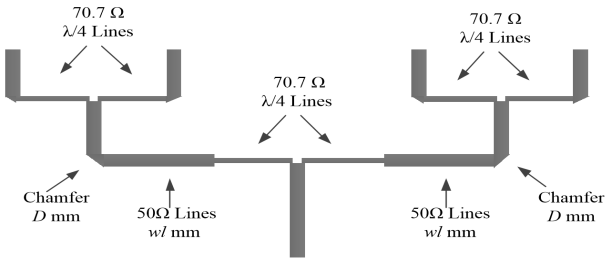

Figure 2. T-Junction network for feeding the 1x4 patch antenna array.
Source: The Authors.

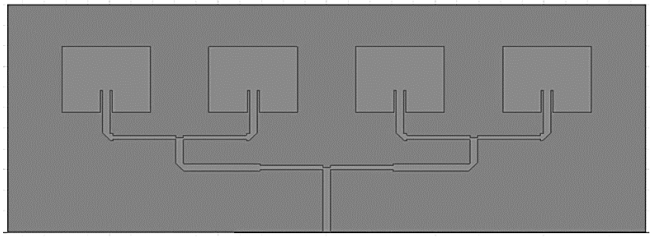

Figure 3. Linear arrangement of 1 × 4 patch antennas obtained after optimization with HFSS.
Source: The Authors.

Table 1.
Geometric and performance parameters of the 1× 4 patch antenna array obtained via simulation using HFSS.

Parameter	Value
Base antenna width (W)	40.7 mm
Base antenna length (L)	32.5mm
Antenna separation (d)	0.55λ
Resonance frequency (f_0)	2.44 GHz
Input impedance (f_0)	50.0812 Ω
3dB-RL bandwidth (VSRW≤1.5)	26.9 MHz
Array gain	10.2736 dB
-3dB horizontal beamwidth	22.4832º

Source: The Authors.

$$M = 52 + 65e^{-1.35\frac{w_l}{h}} \quad (3)$$

Where w_l = 3.84 mm is the width of the 50 Ω line [15]. We reduced the width of the horizontal branches of all T-junctions vertically in the joining point by an amount of 1.34 mm ($\sim 0.6w_l$) in accordance to [13,15].

With these preliminary theoretical geometric values, we proceeded to optimize the 1× 4 patch antenna array by successive simulations in HFSS until the results shown in Fig. 3 and Table 1 were obtained.

As can be seen on Table 1 the simulated array exhibits an input impedance very close to 50 Ω at resonance and a horizontal beamwidth of 22.4832°.

3. Antenna array experimental characterization

With the optimized geometric parameters given in Table 1 we constructed the two patch antenna arrays that are shown in Fig. 4.

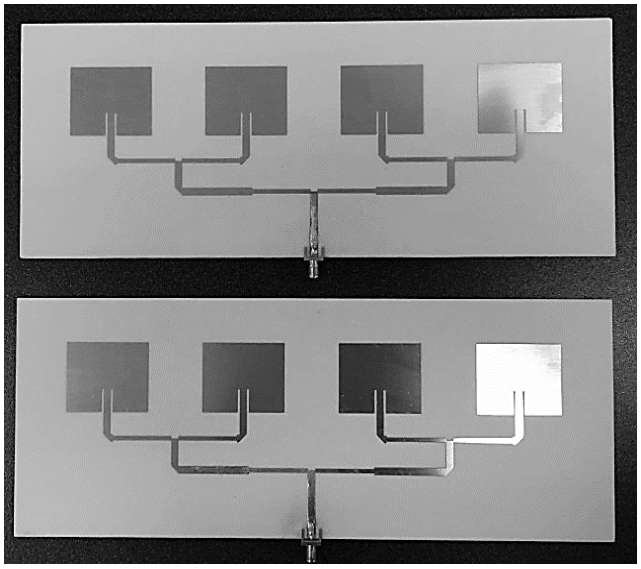

Figure 4. Antenna arrays constructed using the geometric parameters given in Table 1.
Source: The Authors.

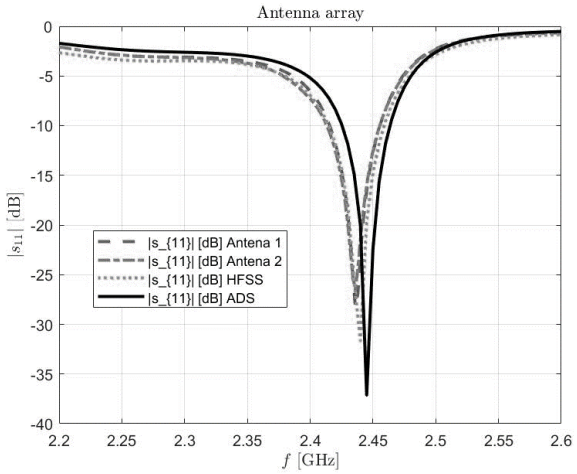

Figure 5. Measured RL and estimated RLs using HFSS and ADS.
Source: The Authors.

Then, we characterized experimentally the constructed antennas in an anechoic chamber. We measured the following parameters of interest: a) the return loss *RL* in the 2.4 to 2.5 GHz band, b) the standing wave ratio *SWR* in the 2.4 to 2.48 GHz band, c) the resonance frequency f_0, d) the bandwidth *BW*, e) the gain, and f) the radiation pattern.

Fig. 5 shows the antenna return loss measured experimentally together with the RLs obtained via simulation using HFSS and ADS.

We can read from Fig. 5 a resonance frequency of f_0 = 2.436 GHz corresponding to the minimum value of $|S_{11}|$.

Fig. 6 shows the measured SWR of both antennas. The antenna bandwidth can be determined from any of Figs. 5 and 6. From Fig. 6 we have estimated a 1.5-SWR bandwidth of BW = 24.0121 MHz.

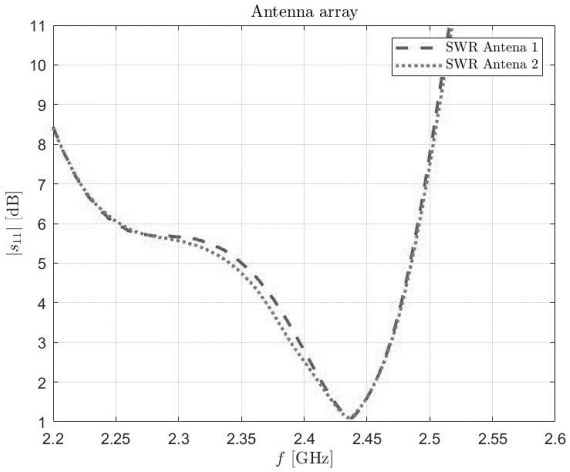

Figure 6. SWR measured on both antennas.
Source: The Authors.

Table 2.
Measured and estimated gain of the antennas.

Measured gain (dB)	Estimated gain (dB) using HFSS	Estimated Gain (dB) using ADS
9.8737	10.2736	10.2061

Source: The Authors.

For estimating the patch antenna array gain (at f_0 = 2.436 GHz), we settled the distance between the antennas to r = 2.05 m, and with the vector network analyzer, we measured a $|S_{21}|$of -26.633 dB. Subsequently, we determined the gain using Equation 17.15 of reference [8]. Table 2 shows the measured gain value of the antennas together with the values estimated using HFSS and ADS.

In the anechoic chamber, we also measured the antenna array radiation pattern and then we plotted the measured pattern together with those estimated by HFSS and ADS. Fig. 7 shows the results obtained.

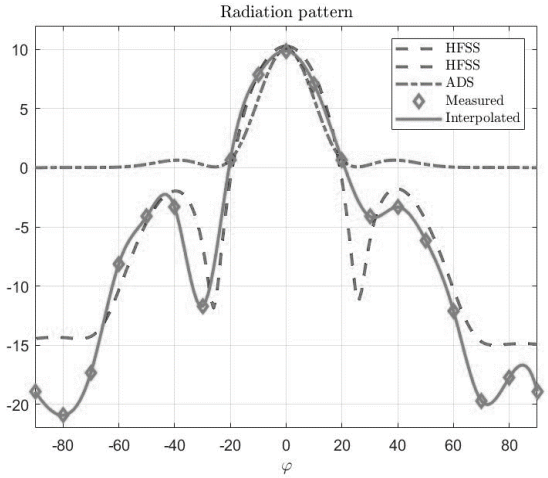

Figure 7. Patch antenna array 2D radiation patterns measured and estimated using HFSS and ADS.
Source: The Authors.

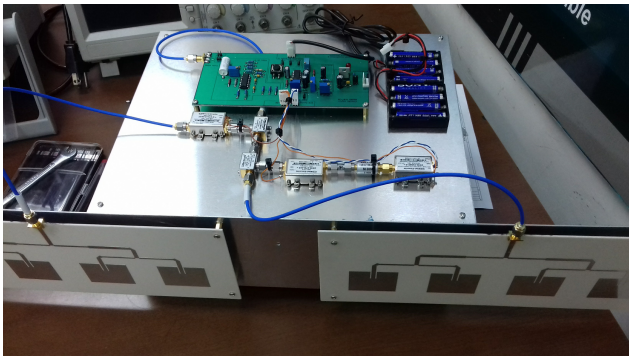

Figure 8. Snapshot of the radar implemented.
Source: The Authors.

4. Antenna performance on the radar

Finally, we incorporated the two implemented antennas described in the previous section to the LFM-CW radar prototype as shown in Fig. 8.

For testing the synthetic aperture radar prototype, we arranged a rectangular polygon of 12m x 100m with four corner reflectors in it as shown in Fig. 9. On one of the shorter side of this polygon, we installed the radar on a rail at a height of 1.2 m above ground, and we slid it following a stop and go scheme whilst taking samples of the echo received every 10 cm.

Next we post-processed the raw data collected by the radar in GNU Octave using the ω-κ algorithm, and we generated an image of the scene inside the polygon as shown in Fig. 10.

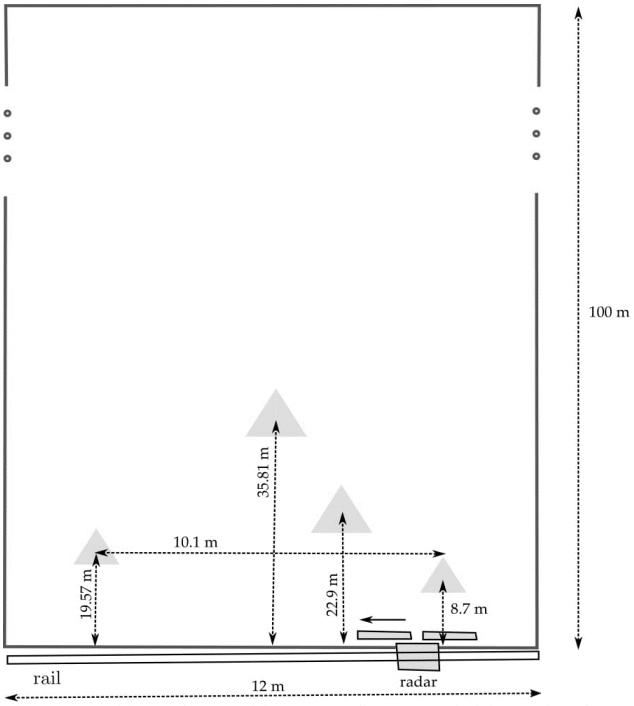

Figure 9. Probing polygon with corner reflectors settled for testing the radar.
Source: The Authors.

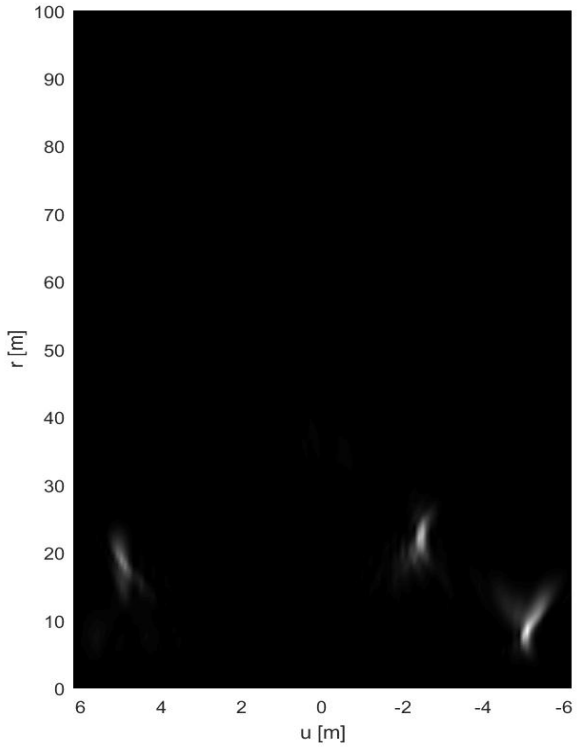

Figure 10. Image generated from raw data collected by the radar using the ω-κ algorithm.
Source: The Authors.

In the image of Fig. 10, we observe three luminous targets corresponding to the three closest corner reflectors in the scene. The farthest target does not appear in the image due to its poor azimuthal phase registration and its 30 dB bigger free space loss.

Afterwards we processed the image on Fig 10 with GNU Octave; we measured graphically the azimuthal width of the sync-like point spread function of each target [4,5]. As the first zero crossing of the sync-like function determines the azimuthal resolution of the radar, we assessed an azimuthal resolution of approximately 0.15m.

By the other hand, as it is well known, the theoretical azimuthal resolution is given by the expression [4]:

$$\delta_H = \frac{\lambda_0}{2\theta_H} \tag{4}$$

where λ_0 is the free-space wavelength at f_0, and $\Delta\theta_H$ is the antenna horizontal beamwidth. By substituting the values of $\lambda_0 = 0.12$m, and $\Delta\theta_H = 0.42$ rads in Eq. (16), we would expect a theoretical azimuthal resolution of $\delta_H = 0.14$m.

5. Acknowledgements

We thank Luis Ledezma, from the Jet Propulsion Laboratory, California Institute of Technology, for comments and suggestions that helped improve this manuscript.

This work was funded by the Prometeo Project of the Secretariat for Higher Education, Science, Technology and Innovation of the Republic of Ecuador.

6. Conclusions

We have built two 1x4 patch antenna arrays for a LFM-CW synthetic aperture radar prototype developed at the Ecuadorian Space Institute (IEE: Instituto Espacial Ecuatoriano).

We installed the arrays in the radar, and we tested the radar in a probing polygon with four corner reflectors, sliding the radar on a rail and using a stop and go scheme. Subsequently, we focused the raw data collected by the radar using the ω-κ algorithm using GNU Octave. As a result, we generated a radar image of the scene inside the polygon. On the image itself, where only the three most luminous targets were correctly focused, we estimated graphically the horizontal resolution of the radar obtaining a value coinciding with the expected theoretical one.

References

[1] Moreira, A., Prats-Iraola, P., Younis, M., Krieger, G., Hajnsek, I. and Papathanassiou, K.P. A tutorial on synthetic aperture radar, IEEE Geoscience and Remote Sensing Magazine, 1(1), pp. 6-43, 2013. DOI: 10.1109/MGRS.2013.2248301

[2] Chan, Y.K. and Koo, V.C., An introduction to synthetic aperture radar (SAR), Progress in Electromagnetics Research B, 2, pp. 27-60, 2008. DOI:10.2528/PIERB07110101

[3] Curlander, J.C. and McDounough, R.N., Synthetic aperture radar, systems and signal processing, Wiley-Interscience, USA, 1991, 672 P.

[4] Sullivan, R.J., Radar foundations for imaging and advanced concepts, Scitech Publishing, Chennai, India, 2004, 476 P. DOI: 10.1049/SBRA030E

[5] Zozaya, A.J., Carrera, F. and Bolaños, R., Radar imaging basics, Revista Ingeniería UC, 24(1), pp. 73-80, 2017. ISSN: 1316-6832

[6] Christensen, E.L. and Dich, M., SAR antenna design for ambiguity an multipath suppression, Proceedings of IGARSS '93 - IEEE International Geoscience and Remote Sensing Symposium, Tokyo, Japan, 1993. DOI: 10.1109/IGARSS.1993.322219

[7] Pokuls, R., Uher, J. and Pozar, D.M., Microstrip antennas for SAR applications, IEEE Transactions on Antennas and Propagation, 46(9), pp. 1289-1296, 1998. DOI: 10.1109/8.719972.

[8] Balanis, A., Antenna theory. Analysis and design, JohnWiley & Sons, Inc., USA, 2005, 1104 P.

[9] Gupta, K.C., Garg, R., Bahl, I. and Bhartia, P., Microstrip lines and slotlines, Artech House, 2nd Ed. 1996, 560 P.

[10] Ansoft, L., An introduction to HFSS: fundamental principles, and use, Ansoft, LLC, Pittsburgh, USA, 2009, 45 P.

[11] Keysight Technologies, Advanced Design System (ADS), 2018. [Online]. [Accessed October 25th of 2018]. Available at: https://www.keysight.com/en/pc-1297113/advanced-design-system-ads?cc=VE&lc=eng.

[12] Pozar, M., Microwave Engineering, JohnWiley & Sons, Inc., 2012.

[13] Pozar, M., Microstrip antennas, Proceedings of the IEEE, 1992. DOI: 10.1109/5.119568

[14] Rogers, R., Corporation, [Online]. [Accessed October 25th of 2018]. Available at: https://www.rogerscorp.com/index.aspx.

[15] Kumar, G., Broadband microstrip antennas, Artech House, Ed., Norwood, Ohio, USA, 2003.

[16] Matin, M.A. and Sayeed, A.I., A design rule for inset-fed rectangular microstrip, WSEAS Transactions on Communications, 9(1), pp. 63-72, 2010. ISSN: 1109-2742

A. Zozaya, received the BSc. in Electronic Engineering, with a major in Telecommunication, in 1991, from the Instituto Universitario Politécnico de las Fuerzas Armadas Nacionales (IUPFAN), Maracay, Venezuela, and PhD in 2002, from the Universidad Politécnica de Cataluña (UPC), Barcelona, Spain, in the area of Signal Theory and Communication. He worked as a professor at the Universidad de Carabobo, Valencia, Venezuela since 1994 to 2014. He worked as a senior researcher at the Ecuadorian Space Institute, Quito, Ecuador, in the area of synthetic aperture radars in the periods from September 2014 to September 2015, and from August 2016 to August 2017. Currently, he is a full professor in the Universidad Tecnológica Metropolitana del Estado de Chile (UTEM), Santiago de Chile, at the Department of Electricity. His research interests include applied electromagnetic, computational electromagnetic, digital signal processing, RF circuits design, and synthetic aperture radars.
ORCID: 0000-0003-3357-3887.

P. Del Pino-Pettinare, is a BSc. in Electrical Engineer, in 1988, and MSc. in Electrical Engineering Telecommunications research area, in 2004, from the University of Carabobo, Valencia, Venezuela. Since 1988 he has worked in different projects in the area of electrical-electronics engineering and in telecommunications, both in the private sector and at the University of Carabobo, Venezuela. He is a full professor at the School of Telecommunications Engineering at the University of Carabobo and his areas of interest in the research are: estimation of SAR and RCS of arbitrary geometry and constitution bodies using MoM and FDTD for applications in microwave imaging and determination of the thermal response of human biological tissue to microwave radiation for medical applications. Optimal estimation of RCS using MoM and MLFMM. Design, construction and characterization of RF and microwave circuits. Design, construction and characterization of antennas. Estimation of coverage and propagation studies in AM / FM broadcasting, and broadcasting in the UHF band.
ORCID: 0000-0003-1451-6086.